Princeton Plasma Physics Laboratory

PPPL- 4768

PPPL- 4768

Intrinsic Rotation Generation in NSTX Ohmic H-mode Plasmas

Jong-Kyu Park, Ronald E. Bell, Stanley M. Kaye, Wayne M. Solomn,
Benoit P. LeBlanc, Ahmed Diallo, and Shigeyuki Kubota

June, 2012

Prepared for the U.S. Department of Energy under Contract DE-AC02-09CH11466.

Princeton Plasma Physics Laboratory
Report Disclaimers

Full Legal Disclaimer

Trademark Disclaimer

PPPL Report Availability

Princeton Plasma Physics Laboratory:

http://www.pppl.gov/techreports.cfm

Office of Scientific and Technical Information (OSTI):

http://www.osti.gov/bridge

Related Links:

U.S. Department of Energy

Office of Scientific and Technical Information

Fusion Links

Intrinsic Rotation Generation in NSTX Ohmic H-mode Plasmas

Jong-Kyu Park,[1] Ronald E. Bell,[1] Stanley M. Kaye,[1] Wayne M. Solomon,[1] Benoit P. LeBlanc,[1] Ahmed Diallo,[1] and Shigeyuki Kubota[2]

[1] *Princeton Plasma Physics Laboratory, Princeton, New Jersey 08543, USA*

[2] *University of California in Los Angeles, Los Angeles, California 90095, USA*

(Dated: June 1, 2012)

Abstract

Intrinsic rotation generation has been observed and investigated in NSTX Ohmic plasmas, by utilizing passive views of charge exchange recombination diagnostics. Particularly we focused Ohmic L-H transition to minimize effects by other momentum exchange and sources such as an intrinsic NTV. Results indicated that intrinsic rotation generation in the edge is well correlated with ion temperature gradient change, compared with much weaker correlations with electron temperature gradient or density gradient change. This is consistent with a corresponding theory of residual stress and the measured torque could be directly compared with the theoretical prediction using χ_i as a free parameter. However, an uncertainty of an order of diamagnetic rotation exists in many places across measurement and theory, as well be discussed in details in this paper.

I. INTRODUCTION

Intrinsic toroidal rotation and torque is an important subject in tokamaks as it is expected to play a dominant role in establishing toroidal rotation in ITER. Toroidal rotation is tightly linked to $\vec{E} \times \vec{B}$ rotation and its shearing rate, which can strongly influence various instabilities from macroscopic scale [1, 2] to microscopic scale [3, 4], and therefore better understanding for intrinsic toroidal rotation can lead to better prediction for stability in ITER.

The terminology of *intrinsic* toroidal rotation typically refers to the finite toroidal rotation in a tokamak even without an external toroidal momentum injection. Obviously there is no momentum injection in Ohmically heated plasmas, but co-I_P toroidal rotation has been observed and reported in Ohmic H-mode discharges in many devices including COMPASS-D [5], CMOD [6–8], DIII-D [9, 10], and TCV. This paper will add another case, but for a Spherical Torus, National Spherical Torus eXperiment (NSTX) [11], by utilizing passive view of charge exchange recombination spectroscopy (CHERS).

The link to the H-mode indicates the relation of the intrinsic rotation to the confined thermal energy, phenomenologically, as now well known by W_P/I_P scaling [12]. The same trends have been found in discharges heated by radio frequency wave heating including ICRF, ECH, and LH (See also Ref. [12]), although the possibility of momentum exchange between waves and high energy particles always exists and so still it is not entirely clear if RF-heated discharges are indeed free from external toroidal momentum injection.

Even in a truly intrinsic situation without toroidal momentum injection, momentum exchange inside plasma or with external system can complicate the determination of the intrinsic part from measured toroidal rotation [13]. Three major components are the momentum diffusion, and the momentum convection or pinch [14, 15], and the momentum damping associated with toroidal asymmetry in magnetic field [16, 17]. Including the intrinsic drive of momentum, these components are often not easily distinguishable from each other and would require the complete profile evolution information of rotation with relevant model for each part.

An innovative method was used in DIII-D, using the fact that the momentum diffusion and pinch effects can be minimized if rotation is removed, and by estimating required NBI torque to balance the intrinsic rotation and thus to maintain the almost zero level of rotation

[18]. This method unfortunately needs the balanced NBI beams, which are not commonly available in other devices. Also even with that advanced method, there is a possibility of the momentum damping by toroidal asymmetry, namely intrinsic Neoclassical Toroidal Viscosity (NTV) [17, 19, 20]. In this study, the focus was made to the intrinsic drive of rotation through a short time period in L-H transition, where we believe the momentum diffusion and pinch effects can be ignored, and also in Ohmic plasmas where the momentum damping by toroidal asymmetry can also be ignored.

Once only the intrinsic part is pulled over from experiments, one can make a comparison with theoretical prediction. One of novel mechanisms predicted in theory is the residual part of Reynolds stress, by the reflection symmetry breaking in the parallel wave vector $k_{||}$ of turbulence [21–23]. This concept can be summarized as a conversion of thermal energy into momentum by drift wave turbulence excited by inhomogeneity in T and n. So eventually the predicted intrinsic drive is proportional to ∇T or ∇n, as will be tested in this study. Other mechanisms, such as geometrical up-down asymmetry [24] or charge separation from the polarization drift [25], are ignored since most of studied discharges are up-down symmetric, and the investigated region is around the pedestal where the residual stress is expected to play a major role.

Note another issue exists in measurement itself, since what is measured is the rotation of impurity ions, not main ions, which therefore should be inferred based on equilibrium flow balance. Main uncertainty in the flow balance is the poloidal rotation of each species, which also should be inferred unless directly measured. Neoclassical theory is commonly used to estimate the poloidal rotation and the flow balance, but uncertainty is probably as large as the intrinsic rotation in both measurement and theory as will be illustrated.

This paper is organized as follows. Section II will describe studied NSTX experiments and the observations for intrinsic rotation during Ohmic L-H transitions, as well as the correlation with ∇T and ∇n. Section III will discuss the torque balance and comparisons with a corresponding theory of residual stress, followed by summary and discussion in Section IV.

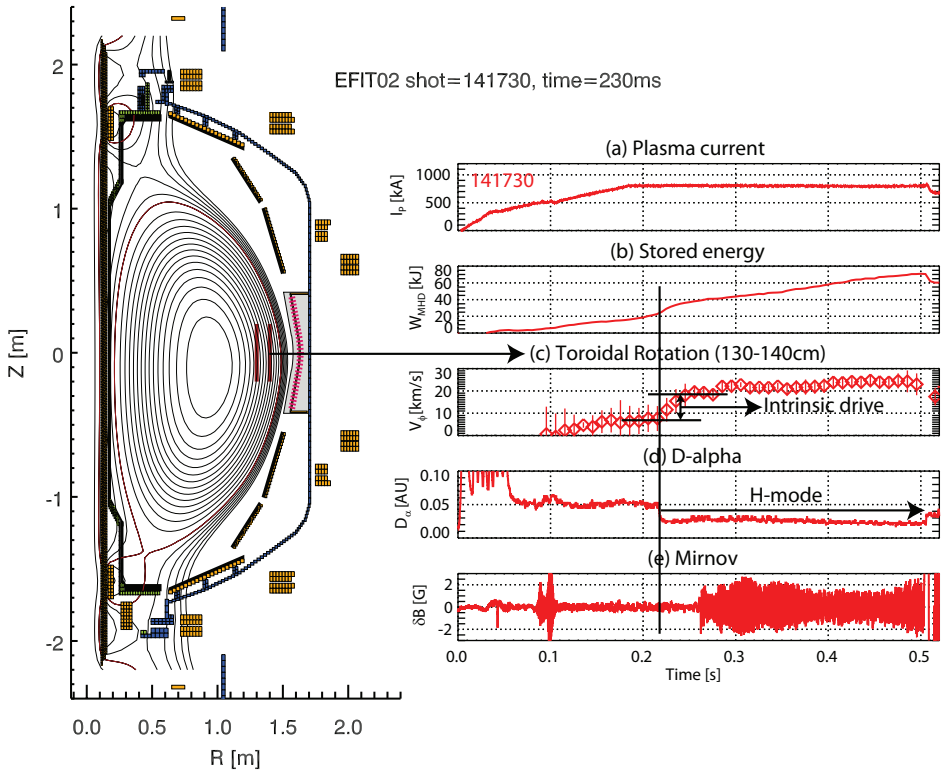

FIG. 1. An example of NSTX Ohmic H-mode discharge (#141730) with time traces for (a) plasma current, (b) stored energy, (c) toroidal rotation, (d) D_α, and (e) Mirnov signal indicating tearing modes later in time. The L-H transition occurred at $t = 220ms$ as indicated by the black vertical line. The toroidal rotation in (c) is the average of the edge rotation in $R = 130cm \sim 140cm$, which was measured by passive views of CHERS. One can see the rapid increase of the toroidal rotation right after the L-H transition.

II. OBSERVATION FOR INTRINSIC ROTATION AND CORRELATION WITH ION TEMPERATURE GRADIENT

The increase of toroidal rotation to the co-I_P direction could be clearly observed in NSTX Ohmic H-mode plasmas, as has been reported in many devices. Figure 1 shows a typical target plasma and a shot trace in experiments as an example. This is an $800kA$ Ohmic discharge, with $\kappa \sim 1.9$, $\delta_{ave} \sim 0.51$, $q_{95} \sim 8.2$, and with almost double-null and so up-down symmetry. A few exceptional cases with up-down asymmetry existed, but no difference was found in results indicating that intrinsic rotation drive by up-down asymmetry is not a dominant mechanism and can be ignored in our study. The shot went into the H-mode at

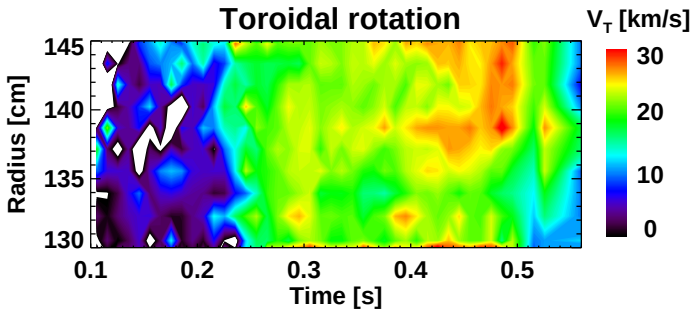

FIG. 2. Evolution of carbon toroidal rotation in the edge, measured by passive views of CHERS. One can see clearly the increase of toroidal rotation after L-H transition $t \sim 0.22s$.

$t \sim 220ms$ and the H-mode was maintained until $t \sim 505ms$ as indicated by D_α signal and also as can be seen in the increase of stored thermal energy. Toroidal rotation measured in the edge showed fairly rapid increase up to $10km/s$, or often almost jump into a different level when viewed by the limited time resolution of rotation measurement, and became steady afterwards.

The steady rotation after about $\sim 30ms$ of L-H transition is somewhat inconsistent with the continuous increase of thermal energy after the transition, i.e., W/I_P scaling. One feasible explanation for it in this case is that a damping by tearing mode might be involved as can be seen by Mirnov signals. A low torque plasma provides better circumstances to study intrinsic rotation, but may be vulnerable to MHD modes, which can give an additional momentum transport associated with modes. Our study excluded those cases or the periods of MHD modes to avoid the complication in the analysis. Another possibility is the momentum inward pinch, which can transfer the intrinsic torque in the edge to the core until balanced with momentum diffusion, etc. These momentum exchange effects can be minimized in a short time period right after L-H transition as long as the momentum confinement time is longer than the studied period. Also normally at this time, MHD mode does not appear either, possibly because L-H transition by only Ohmic heating may become more difficult when MHD mode exists in the first place.

In principle, momentum exchange effects can be studied together with intrinsic torque if profile evolution is fairly well resolved in space and time. This is often limited in the measurement of toroidal rotation without NBI, as is the case in our study. We used the passive view of charge exchange recombination spectroscopy (CHERS), which measures the background and plume C^{5+} ions and gives their toroidal rotation by inverting line-integrated

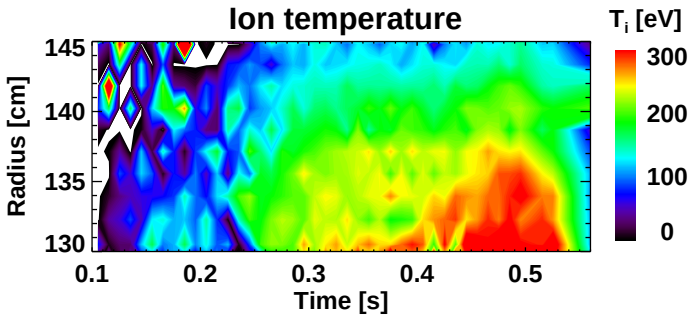

FIG. 3. Evolution of ion temperature in the edge, measured by passive views of CHERS. One can see also the clear increase of ion temperature after L-H transition $t \sim 0.22s$, but there is the difference in the spatial profile compared to the toroidal rotation in Figure 2.

values by 63 pairs of sightlines [26]. Because the emissivity for those background ions is not strong enough in the core, so the reliability of measurement is limited in the edge region. Comparing the information from passive CHERS with active CHERS in a different shot with NBI blips, one can find good agreement in the edge, $130 \sim 145cm$, or equivalently $0.60 < \psi_N < 0.95$.

Figure 2 shows an example of the passive CHERS measurement for toroidal rotation, in the edge $130 \sim 145cm$ measured along the time. A H-mode was achieved and maintained at $t > 220ms$ in this discharge, as shown in Figure 1, and one can see the apparent increase of toroidal rotation during H-mode phase until $t \sim 505ms$. As introduced already, one of the goals in this study is to find correlations with temperature or density gradient, and thus ion temperature profile evolution is also investigated using the passive CHERS as shown in Figure 3. An interesting feature can be unveiled if one compares Figures 2 with 3 and notices that their peaks are located differently in general and the possibility of correlation between rotation and ion temperature gradient.

The information of the profile gradient is harder than the profile itself due to various error sources in measurement and inversion of diagnostic data. Especially noises upon the overall envelope should be eliminated by smooth fitting. We selected 4 spatial points at $R = 132, 136, 140, 144cm$ and obtain the quantity and the gradient by taking average around each point without an overlap. Errors then of course will be accumulated and propagated, from the emissivity, the inversion, to the finally obtained profile, but the level is tolerable as will be shown later. For electron temperature and density, multi-point Thomson scattering

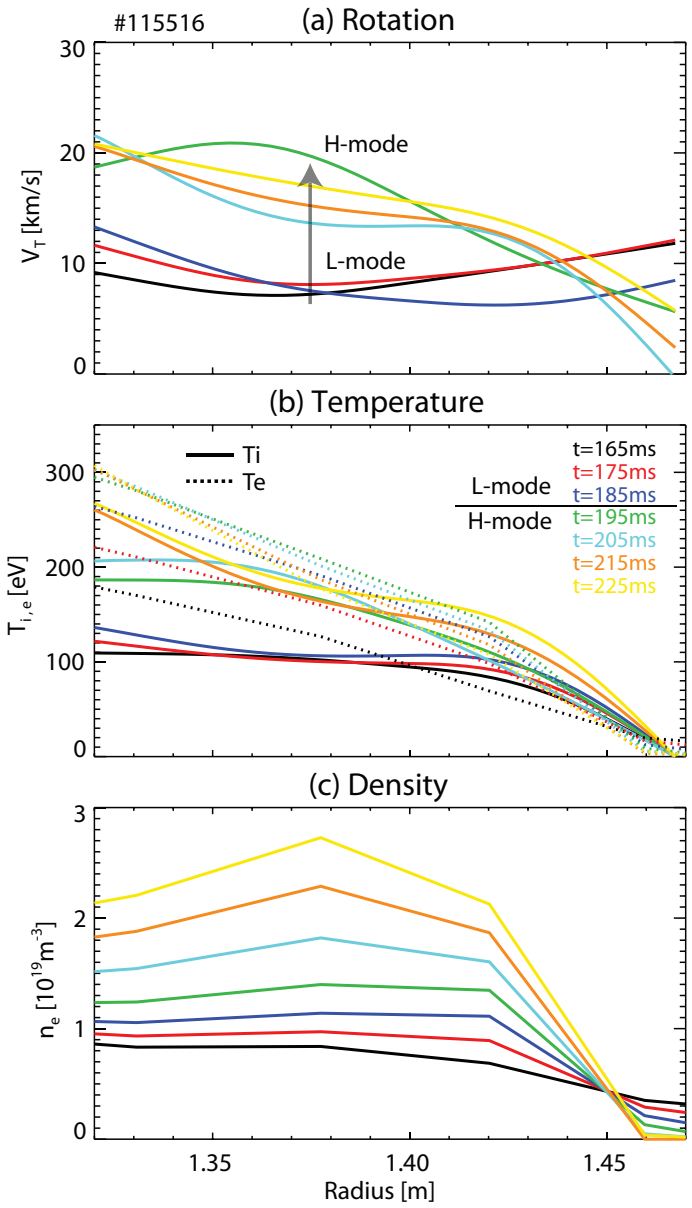

FIG. 4. Edge profiles of rotation, temperature, and density after the smoothed fits that are necessary to take the gradient information. Note the separatrix is located at $R = 1.46m$, and the magnetic axis $R \sim 1.0m$ is far from the left. Passive CHERS becomes unreliable with larger errors in $R < 1.30m$. The time resolution is limited by $\Delta t \sim 10ms$. One can see clearly the rapid change in toroidal rotation and ion temperature through L-H transition ($t = 185ms \rightarrow t = 195ms$).

is much more reliable with small errors, but only the same 4 spatial points were selected and averaged for comparison.

An example of results is shown in Figure 4. It shows the edge profile evolution of toroidal

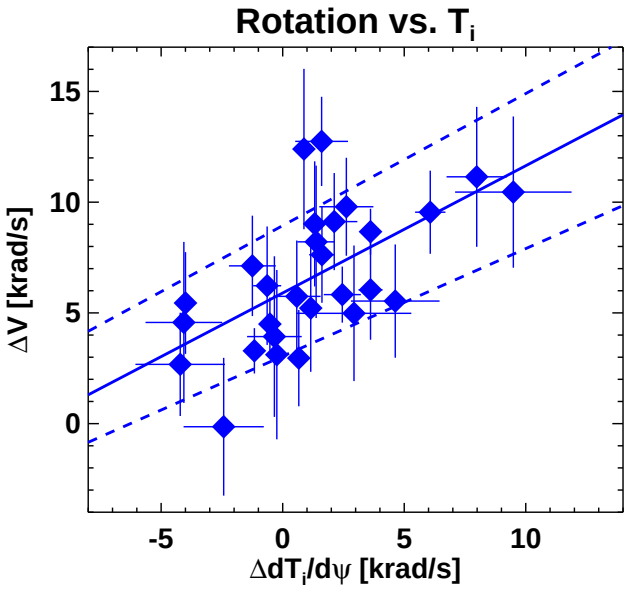

FIG. 5. Correlation between the measured changes of carbon toroidal rotation and ion temperature through L-H transition. One can find $\Delta V_{Ex} = C_z \Delta V_d$ with $C_z \approx 0.57$ in average with an offset $\sim 5km/s$. There is a reasonable positive correlation compared to Figure 6.

rotation, ion and electron temperature, and electron density in 3 different time slices in L-mode ($t = 165, 175, 185ms$) and 4 different time slides in H-mode ($t = 195, 205, 215, 225ms$). One can see very rapid changes in toroidal rotation $V \equiv V_\phi$ and ion temperature T_i profiles through L-H transition, compared to electron temperature T_e or density n_e profiles. Moreover, the greatest change in V occurs at $R < 1.42m$, where is deeper to the core than the density pedestal. In fact, one can see that the increase of T_e or n_e is largely driven by each gradient increase in the density pedestal, while T_i increases along with broader gradient increase which might be correlated with the increase of V. Note it is quite surprising that a very large change of V occurs within $10ms$ after L-H transition, but unfortunately, $10ms$ was our smallest time resolution used in experiments and so dynamics in such a short time period could not be studied.

Using the smoothed profiles, correlation studies were performed over about ~ 10 Ohmic H-mode discharges in NSTX 2005$\sim$2011 operation. At 4 selected points for each shot, we compared the change of toroidal rotation ΔV with the change of temperature and density gradient $\Delta(dT/d\psi)$ and $\Delta(T/n)(dn/d\psi)$ in $10ms$ around L-H transition. The reason why the *change* is measured in a short time period is again to minimize other momentum exchange

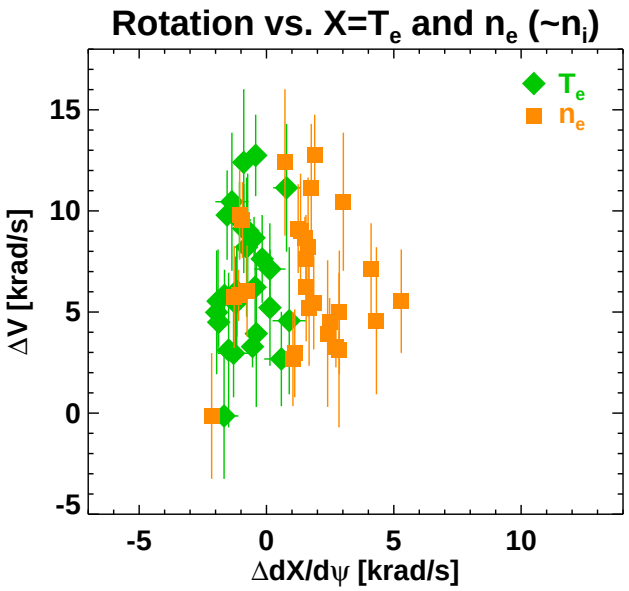

FIG. 6. Correlation between the measured changes of carbon toroidal rotation and electron temperature (Green diamond) and density (Orange square) through L-H transition. There is no apparent correlation found.

effects, which will be further discussed later with torque balance issues.

As the possibility was discussed in profile evolutions, the best correlation was found indeed with ion temperature gradient, as in Figure 5. In average we found

$$\Delta V_{Ex} = C_z \Delta V_d \tag{1}$$

with $C_z \approx 0.57$, where a diamagnetic-like speed V_d is defined as

$$V_d \equiv R dT/d\psi. \tag{2}$$

This is convenient in experimental point of view since $dT/d\psi$ becomes in units of rad/s when units of $T[eV]$ and the poloidal flux function $\psi = \psi_{\rm pol}/2\pi$ are used. Note the offset up to $5km/s$ within error bars. An offset was also found in recent DIII-D results [18]. Correlations with electron temperature and density are much poor, as shown in Figure 6, because the gradient change for $dT_e/d\psi$ and $dn_e/d\psi$ is not spatially aligned with the change for V. Here ion density profile n_i is not shown since impurity profiles are not available and so cannot be compared. Nonetheless a test shot with NBI blips indicated $n_e \sim n_i$ only with $\sim 5\%$ difference, so we conclude that the only ion temperature gradient shows the relevant correlation with intrinsic toroidal rotation through L-H transition.

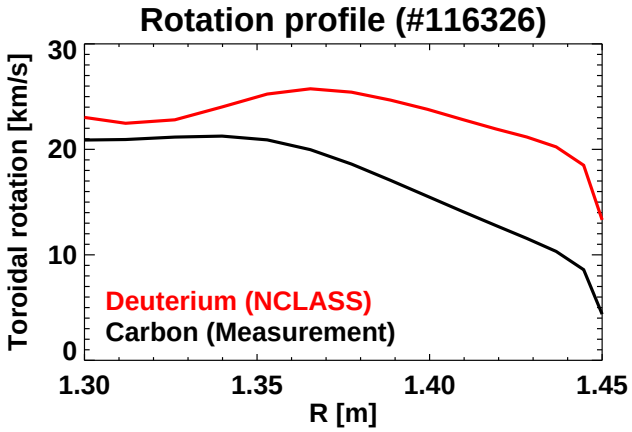

FIG. 7. NCLASS prediction for the main ion toroidal rotation using the measured impurity toroidal rotation as an example (#116326 at $t = 195ms$). $Z_{\text{eff}} = 1.5$ is assumed.

The correlation with the ion temperature gradient is consistent with theoretical prediction. Before making comparison, however, it is necessary to discuss the difference between the *impurity rotation* V_z measured and the *main ion rotation* V_i. Considering the flow balance for each species [27]

$$V_s \cdot \nabla\phi = -\left(\frac{d\Phi}{d\psi} + \frac{1}{Z_s e n_s}\frac{dP_s}{d\psi} - qV_s \cdot \nabla\theta\right), \tag{3}$$

where the contribution from the poloidal rotation is $qV_s \cdot \nabla\theta = (I/R^2)(V_{s\theta}/B_\theta)$ with $I = RB_\phi$. So the difference in toroidal rotation between V_z and V_i is given by

$$V_i \cdot \nabla\phi - V_z \cdot \nabla\phi = -\left(\frac{1}{en_i}\frac{dP_i}{d\psi} - \frac{1}{Zen_z}\frac{dP_z}{d\psi}\right) + \frac{I}{R^2}\left(\frac{V_{i\theta}}{B_\theta} - \frac{V_{z\theta}}{B_\theta}\right). \tag{4}$$

The impurity diamagnetic rotation can be ignored in most cases, so the difference becomes the difference in the poloidal rotation in addition to the ion diamagnetic rotation. One way to evaluate the poloidal rotation when it is not directly measured is to use neoclassical theory. A few cases were tested with TRANSP and NCLASS [28, 29] by assuming $Z_{\text{eff}} = 1.5$ based on NBI blip shot data, as an example shown in Figure 7 at a time slice right after L-H transition.

One can see the significant difference in main ion rotation $R > 1.35m$, up to a factor of 2. In principle, one can run NCLASS for every case to find out the prediction for the main ion rotation. Many assumptions should however be needed, such as carbon and impurity

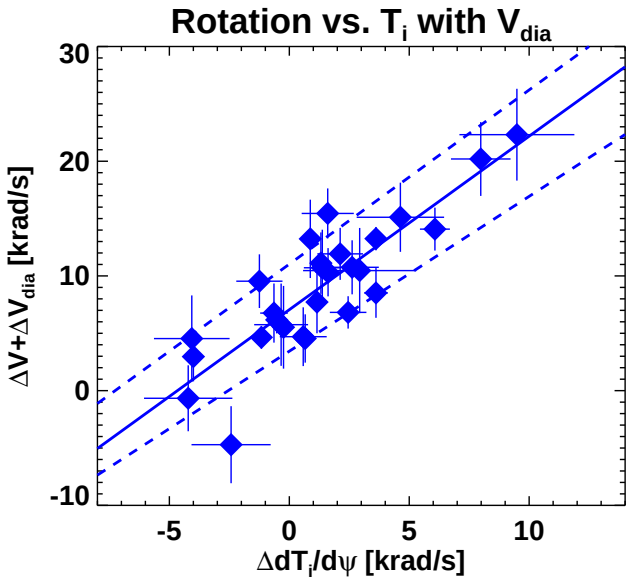

FIG. 8. Revised correlation with ion temperature gradient for the main ion rotation, which is calculated by neoclassical flow balance ignoring the poloidal rotation [26] and impurity pressure. As a result, the toroidal rotation change is increased by diamagnetic rotation change.

III. TORQUE BALANCE AND COMPARISON WITH THEORY

The increase of the toroidal rotation without an external torque is driven by intrinsic toroidal torque. The intrinsic torque is more fundamental mechanism and the rotation is the consequence of the torque balance between the momentum exchange. For comparison with experiments, consider the torque balance in a cylindrical limit,

$$\frac{\partial MnRV}{\partial t} = T_{input} - \nabla \cdot \Pi^{3D}_{r\phi} + \nabla \cdot \Pi_{r\phi}, \tag{6}$$

where

$$\Pi_{r\phi} = MnR\left(\chi_\phi \frac{dV}{dr} - V_{pinch}V + \Pi^{ex}_{r\phi}\right). \tag{7}$$

Obviously $T_{input} = 0$ in Ohmic plasmas. The torque by 3D field $\nabla\cdot\Pi^{3D}_{r\phi}$ includes the resonant electromagnetic torque at the rational surfaces when tearing mode exists and also Neoclassical Toroidal Viscosity (NTV) torque [17, 19, 20] if axisymmetry is broken. Especially NTV torque almost always exists in tokamaks due to intrinsic asymmetry in the magnetic field, and it would not be ignorable especially for a low torque plasma, where an intrinsic torque can play an important role. This *intrinsic error torque* is however small in Ohmic plasmas, due to the low pressure and the high collisionality, and can be ignored in our studies. Actual

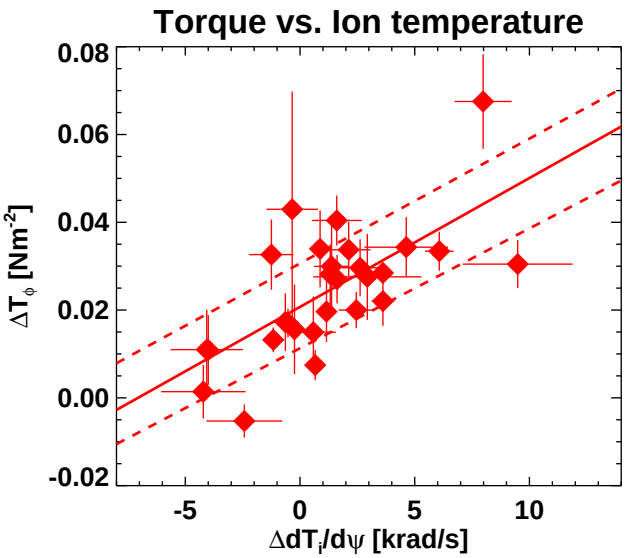

FIG. 9. Correlation between measured torque (density) change and ion temperature gradient change through L-H transition. This torque generation is likely to be purely intrinsic.

modeling is presented in Appendix.

Now if one assumes $-mnRV/\tau_\phi = \nabla \cdot (mnR\chi_\phi dV/dr - mnRV_{pinch}V)$ with momentum confinement time $\tau_\phi >> 10ms$ based on previous NSTX momentum transport studies [13], dominant terms through L-H transition within $\Delta t \sim 10ms$ are

$$\frac{\Delta(MnRV)}{\Delta t} \approx T_\phi^{ex}. \tag{8}$$

So, the increase of the toroidal rotation in our experiments can be regarded as the drive by pure intrinsic torque change. Including the diamagnetic correction, one can study the correlation between the intrinsic torque and the ion temperature change as shown in Figure 9, and obtains

$$T_\phi^{ex} = C_{ex} nRV_d, \tag{9}$$

where $C_{ex} \approx 2 \times 10^{-2}(1 + C_z)$ when units $n[10^{20}m^{-3}]$ and $V_d[km/s]$ are used. Note that Δ can be dropped at this point, by assuming the relation holds from $V_d \to 0$. Here we keep the dependency on the density and the size, as they tend to be natural in a torque density calculation.

The correlation with $V_d \equiv RdT_i/d\psi$ implies the process of intrinsic rotation drive is essentially associated with ion-temperature-gradient (ITG) driven modes, as has been proposed theoretically [21, 22] and experimentally in CMOD [32]. If ITG is the dominant instability

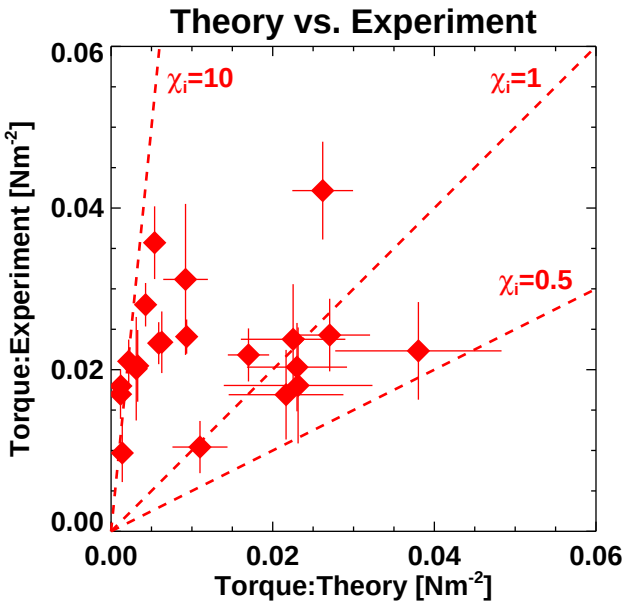

FIG. 10. Comparison between residual-stress theory prediction and measurement for torque density, using χ_i as a free parameter. In theory, higher order temperature variations than T' and toroidal effects are ignored.

source and if $\vec{E} \times \vec{B}$ shearing rate balances the entropy production from ITG in a stationary state, one can estimate the residual stress by $\vec{E} \times \vec{B}$ shearing rate and the intrinsic flow in a stationary state. Diamond obtained the residual stress as [22]

$$\Pi_{r||}^{rs} = -\rho_* \chi_i \frac{L_s}{2c_s} \left(\frac{\nabla T}{T} \right)^2 v_{\text{thi}}^2, \tag{10}$$

where the normalized ion sound Larmor radius $\rho_* = \rho_s/a$, ion sound speed $c_s = \sqrt{T_e/M}$, shear length $L_s^{-1} = \hat{s}/qR$, ion diffusivity χ_i, and thermal ion speed $v_{\text{thi}} = \sqrt{T_i/M}$. Ignoring other spatial variations and higher-order spatial temperature variations than T', and taking a cylindrical approximation, i.e. $\hat{\phi} \sim \hat{b}$, one can obtain the theoretical intrinsic torque density as

$$T_\phi^{rs} = \frac{Mn\epsilon R \chi_i}{2\hat{s} L_T^2} V_d, \tag{11}$$

Then this becomes consistent with observation as they both are correlated with the ion temperature gradient ∇T. For deuterium ions and adopting previous units again, one has

$$T_\phi^{rs} = C_{rs} n R V_d, \tag{12}$$

where $C_{rs} = 1.67 \times 10^{-4} (\epsilon/\hat{s} L_T^2) \chi_i$. Comparing Equations 9 and 12, one can see that theory and experiment can be quantitatively compared if χ_i is used for a free parameter, as shown

in Equation 10. The variation of $\chi_i > 0.5$ is wide, but the range is consistent with previous NSTX momentum transport studies [33]. In principle, χ_i can be estimated with TRANSP by assuming some kinetic profiles that are not available in our study. However, several tests showed that χ_i's based on TRANSP does not seem to well represent the χ_i's based on Figure 10 probably due to various approximations such as $T'' = 0$ as well as unavailable profiles such as $Z_{\rm eff}$. Only the overall range for χ_i seems to agree. Also note the measured and predicted torque density in NSTX is small just due to $\propto nR$ that does not affect the determination of rotation in intrinsic environment, as can be seen from Equation 7.

The prediction of toroidal rotation by intrinsic torque is another important issue, but is not straightforward even if the intrinsic torque can be well predicted. This is beyond the scope of this paper, but it is interesting to consider the consequence of the theory, Equation 10. When there is no other torque than the Reynold stress term in Equation 6, one can use $-\chi_\phi^{\rm eff}\langle V_\phi\rangle' + \Pi_{r\phi}^{rs} = 0$ in a stationary state. Again ignoring other variation and high order temperature variation, one can integrate it and obtain

$$\frac{\langle V_\phi\rangle}{v_{\rm thi}} \cong \frac{1}{2}\rho_* \frac{\chi_i}{\chi_\phi^{\rm eff}} \frac{L_s}{L_T}\sqrt{\frac{T_i}{T_e}}, \tag{13}$$

as obtained by Kosuga [34]. Simplifying the equation, one can see that it becomes

$$\langle V_\phi\rangle \cong \frac{1}{2\hat{s}{\rm Pr}} V_d, \tag{14}$$

where ${\rm Pr} \equiv \chi_\phi^{\rm eff}/\chi_i$. If Pr is an order of unity, ${\rm Pr} \sim 1$, the predicted rotation is possibly much less than the diamagnetic rotation $\sim V_d$. This is highly unfavorable and even it will be very difficult to resolve it in experiments due to the neoclassical uncertainties as discussed in the previous section. If a higher toroidal rotation than a diamagnetic level is desired to avoid various instability, a small ${\rm Pr} < 1/(2\hat{s})$ is required, or otherwise another torque driver will be necessary.

IV. SUMMARY AND DISCUSSION

This paper reported an investigation of intrinsic rotation in NSTX Ohmic H-mode plasmas and a comparison with a corresponding theory of residual stress. Results and issues can be summarized as follows.

1. Experimentally, the increase of toroidal rotation, by $\sim 10km/s$ to the co-I_P direction, could be clearly observed during L-H transition without any external toroidal momentum injection.

2. Passive views of CHERS provided essential measurements in the edge region and indicated the best correlation between the increase of toroidal rotation and ion temperature gradient as $\Delta V_{Ex} = C_z \Delta V_d$, Equation 1.

3. However, the difference between impurity ions and main ions should be corrected. In NSTX, the poloidal rotation may be ignorable and then the flow balance indicated $\Delta V_{Ex} = (1 + C_z)\Delta V_d$. The neoclassical uncertainties, represented by the order of unity 1 is as large as measured intrinsic rotation and so resolution of the rotational difference between species will be equally important.

4. A rotation measurement would not guarantee a torque measurement, so other torque sources should be carefully considered. Our experiments are almost free from momentum pinch, diffusion, and NTV damping effects and so give the information of pure intrinsic torque as $T_\phi^{ex} = C_{ex} nRV_d$, Equation 9.

5. A theory based on residual stress can be simplified as $T_\phi^{rs} = C_{rs} nRV_d$, Equation 12, and a good comparison could be made using χ_i as a free parameter.

6. However, there are a couple of important issues. First, all of discussions in this paper are based on a large-aspect-ratio geometry, which may be not so relevant in a Spherical Torus, and toroidal effects should be accounted in the future.

7. More important issue is that theory originally predicts the residual stress including $(\nabla T)^2$ and so the torque density involves higher order temperature-gradient dependency, such as $(T')^2$ and T''. Our experiments showed only the correlation with T', but the resolution in measurements was not good enough to pin it down and may be embedded in our free parameter χ_i. A very high spatial resolution in measurements will be challenging without NBI, but seems necessary to resolve the higher order dependency.

8. The determination of rotation is a different issue since it additionally requires the information of momentum pinch and diffusion. The corresponding theory predicts

$V \cong (1/2\hat{s}\mathrm{Pr})V_d$, which is less than or equal to the diamagnetic level, as experimentally indicated. Small Pr is required or other momentum sources seems necessary to achieve the rotation higher than the diamagnetic rotation.

In the future work, it will be also important to consider how the intrinsic toroidal rotation can modify $\vec{E}\times\vec{B}$ rotation, which is the ultimate target in the study of the intrinsic rotation. This part in fact constructs the closed loop among $\vec{E}\times\vec{B}$, the intrinsic torque, and the toroidal rotation. Note that the presented theory of the residual stress begins with $\vec{E}\times\vec{B}$ and assumes the intrinsic flow as the next order. It will be desirable to remove the assumption and incorporate other novel mechanisms such as the intensity gradient, since all of pieces involved in the determination of intrinsic rotation may be in a similar order of diamagnetic rotation.

ACKNOWLEDGMENTS

This work was supported by DOE contract DE-AC02-09CH11466 (PPPL).

Appendix: Intrinsic Neoclassical Toroidal Viscosity torque in NSTX Ohmic H-mode

In this appendix a calculation of torque by intrinsic error field in NSTX will be presented. Intrinsic error field almost always exists in tokamaks due to imperfect axisymmetry and can induce a toroidal torque by non-ambipolar momentum transport. This so-called intrinsic neoclassical toroidal viscosity (NTV) torque can be important in a low torque and slowly rotating plasmas, depending on the level of error field and collisionality.

In NSTX, there are two well-known error fields, by the distortion of the centerstack and by the non-circularity of PF5 coils. The developed models for both sources have been well validated in previous studies and so used to calculate non-axisymmetric variation in the field strength including ideal plasma response. The result for $n = 1$ δB calculated by ideal perturbed equilibrium code (IPEC) [35] is shown in Figure 11. One can see clearly the effects of large error field at the inboard side due to the centerstack distortion, as well as small deviations at the outboard side due to PF5 coil errors [36, 37]. In fact $n = 3$ components is larger than $n = 1$ in PF5 coil errors, but can be ignored compared to large

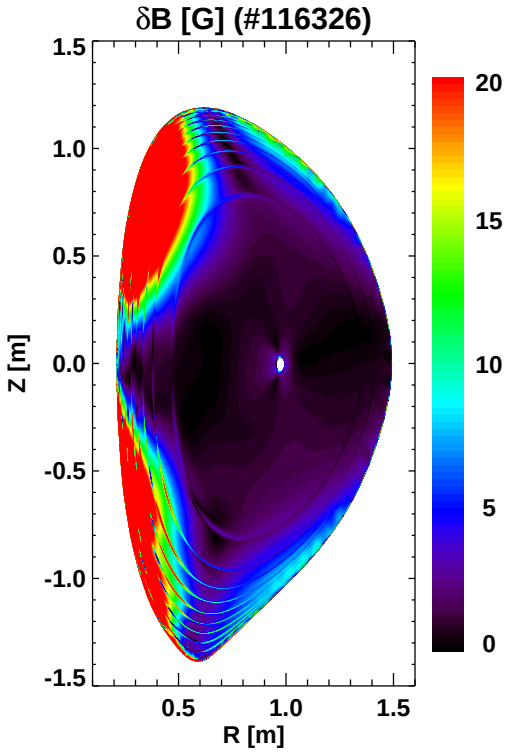

FIG. 11. An example of Lagrangian variation in the field strength δB (#116326 at $t = 195ms$), calculated by IPEC, using the $n = 1$ intrinsic error field model in NSTX. One can see clearly the large error field at the inboard side by centerstack distortion, and the small error at the outboard side by non-circular PF coils.

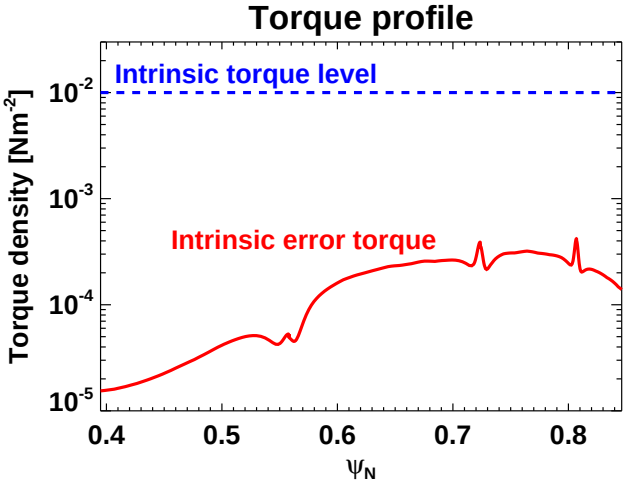

FIG. 12. Calculated torque density profile produced by intrinsic error field, using IPEC δB and combined NTV formula. One can see the *intrinsic error torque* (Red) is small and can be ignored, compared to the measured *intrinsic torque* (Blue), as typical in low temperature Ohmic plasmas.

centerstack distortion in Ohmic plasmas and even were corrected by error field correction (EFC) coils in a few cases.

Using the IPEC δB, we used a combined NTV formulation [20] to calculate the intrinsic NTV torque as this method has been validated in many cases within an order of magnitude [38–40]. The result, Figure 12 shows that the intrinsic NTV torque is much less than the measured intrinsic torque. Therefore we entirely neglected the intrinsic NTV torque in investigation, but note that this should not be generalized to other studies. In fact, two primary reasons of our low NTV torque are the low pressure and the high collisionality in Ohmic plasmas. The low pressure decreases the Lagrangian variation in the field strength as well as the plasma response, and the high collisionality decreases the non-ambipolar transport in $1/\nu$ regime. Considering the NTV torque is proportional to $(\delta B)^2$, one can easily find $\nabla \cdot \Pi^{3D}_{r\phi}$ can increase very rapidly along the temperature [20]. That is, the intrinsic NTV torque can be important when a high confinement with high temperature is targeted without a low external torque, as is the case in ITER.

---

[1] E. J. Strait, T. S. Taylor, A. D. Turnbull, J. R. Ferron, L. L. Lao, B. Rice, O. Sauter, S. J. Thompson, and D. Wróblewski, Phys. Rev. Lett. **74**, 2483 (1995).

[2] S. A. Sabbagh, R. E. Bell, J. E. Menard, D. A. Gates, A. C. Sontag, J. M. Bialek, B. P. LeBlanc, F. M. Levinton, K. Tritz, and H. Yuh, Phys. Rev. Lett. **97**, 045004 (2006).

[3] K. H. Burrell, Phys. Plasmas **4**, 1499 (1997).

[4] S. M. Kaye, R. E. Bell, D. Gates, B. P. LeBlanc, F. M. Levinton, J. E. Menard, D. Mueller, G. Rewoldt, S. A. Sabbagh, W. Wang, and H. Yuh, Phys. Rev. Lett. **98**, 175002 (2007).

[5] Coffey I. H., et al., in *Proceedings of the the 11th Colloquium on UV and x-ray Spectroscopy of Astrophysical and Laboratory Plasmas, and Fronteirs Science Series*, Vol. 15 (Universal Academy, Nagoya, Japan, 1996).

[6] J. Rice, P. Bonoli, J. Goetz, M. Greenwald, I. Hutchinson, E. Marmar, M. Porkolab, S. Wolfe, S. Wukitch, and C. Chang, Nucl. Fusion **39**, 1175 (1999).

[7] I. H. Hutchinson, J. E. Rice, R. S. Granetz, and J. A. Snipes, Phys. Rev. Lett. **84**, 3330 (2000).

[8] J. Rice, J. A. Goetz, R. S. Granetz, M. J. Greenwald, A. E. Hubbard, I. H. Hutchinson, E. S.

Marmar, D. Mossessian, T. Sunn Pedersen, J. A. Snipes, J. L. Terry, and S. M. Wolfe, Phys. Plasmas **7**, 1825 (2000).

[9] J. S. deGrassie, K. H. Burrell, L. R. Baylor, W. Houlberg, and J. Lohr, Phys. Plasmas **11**, 4313 (2004).

[10] J. S. deGrassie, J. E. Rice, K. H. Burrell, R. J. Groebner, and W. M. Solomon, Phys. Plasmas **14**, 056115 (2007).

[11] M. Ono, S. Kaye, Y.-K. Peng, G. Barnes, W. Blanchard, M. Carter, J. Chrzanowski, L. Dudek, R. Ewig, D. Gates, R. Hatcher, T. Jarboe, S. Jardin, D. Johnson, R. Kaita, M. Kalish, C. Kessel, H. Kugel, R. Maingi, R. Majeski, J. Manickam, B. McCormack, J. E. Menard, D. Mueller, B. Nelson, B. Nelson, C. Neumeyer, G. Oliaro, F. Paoletti, R. Parsells, E. Perry, N. Pomphrey, S. Ramakrishnan, R. Raman, G. Rewoldt, J. Robinson, A. Roquemore, P. Ryan, S. A. Sabbagh, D. Swain, E. Synakowski, M. Viola, M. Williams, J. Wilson, and the NSTX Team, Nucl. Fusion **40**, 557 (2000).

[12] J. Rice, A. Ince-Cushman, J. deGrassie, L.-G. Eriksson, Y. Sakamoto, A. Scarabosio, A. Bortolon, K. Burrell, B. Duval, C. Fenzi-Bonizec, M. Greenwald, R. Groebner, G. Hoang, Y. Koide, E. Marmar, A. Pochelon, and Y. Podpaly, Nucl. Fusion **47**, 1618 (2007).

[13] W. M. Solomon, S. M. Kaye, R. E. Bell, B. P. LeBlanc, J. E. Menard, G. Rewoldt, and W. Wang, Phys. Rev. Lett. **101**, 065004 (2008).

[14] A. G. Peeters, C. Angioni, and D. Strintzi, Phys. Rev. Lett. **98**, 265003 (2007).

[15] T. S. Hahm, P. H. Diamond, O. D. Gurcan, and G. Rewoldt, Phys. Plasmas **15**, 055902 (2008).

[16] R. Linsker and A. H. Boozer, Phys. Fluids **25**, 143 (1982).

[17] K. C. Shaing, Phys. Fluids **26**, 3315 (1983).

[18] W. M. Solomon, K. H. Burrell, A. M. Garofalo, S. M. Kaye, R. E. Bell, A. J. Cole, J. S. deGrassie, P. H. Diamond, T. S. Hahm, G. L. Jackson, M. J. Lanctot, C. C. Petty, H. Reimerdes, S. A. Sabbagh, E. J. Strait, T. Tala, , and R. E. Waltz, Phys. Plasmas **17**, 056108 (2010).

[19] K. C. Shaing, Phys. Plasmas **10**, 1443 (2003).

[20] J.-K. Park, A. H. Boozer, and J. E. Menard, Phys. Rev. Lett. **102**, 065002 (2009).

[21] O. D. Gurcan, P. H. Diamond, T. S. Hahm, and R. Singh, Phys. Plasmas **14**, 042306 (2007).

[22] P. H. Diamond, C. J. McDevitt, and O. D. Gurcan, Phys. Plasmas **15**, 012303 (2008).

[23] P. H. Diamond, C. J. McDevitt, O. D. Gurcan, T. S. Hahm, W. X. Wang, E. S. Yoon,

K. Holod, Z. Lin, V. Naulin, and R. Singh, Nucl. Fusion **49**, 045002 (2009).

[24] Y. Camenen, A. G. Peeters, C. Angioni, F. J. Casson, W. A. Hornsby, A. P. Snodin, and D. Strintzi, Phys. Rev. Lett. **102**, 125001 (2009).

[25] C. J. McDevitt, P. H. Diamond, O. D. Gurcan, and T. S. Hahm, Phys. Plasmas **16**, 052302 (2008).

[26] R. E. Bell, R. Andre, S. M. Kaye, R. A. Kolesnikov, B. P. LeBlanc, G. Rewoldt, W. X. Wang, and S. A. Sabbagh, Phys. Plasmas **17**, 082507 (2010).

[27] F. L. Hinton and R. D. Hazeltine, Rev. Mod. Phys. **48**, 239 (1976).

[28] S. P. Hirshman and D. J. Sigma, Nucl. Fusion **21**, 1079 (1981).

[29] W. A. Houlberg, K. S. Shaing, S. P. Hirshman, and M. C. Zanstroff, Phys. Plasmas **4**, 3230 (1997).

[30] G. Kagan and P. J. Catto, Phys. Rev. Lett. **105**, 045002 (2010).

[31] B. A. Grierson, K. H. Burrell, W. W. Heidbrink, M. J. Lanctot, N. A. Pablant, and W. M. Solomon, Phys. Plasmas **19**, 056107 (2012).

[32] J. E. Rice, J. W. Hughes, P. H. Diamond, Y. Kosuga, Y. A. Podplay, M. L. Reinke, M. J. Greenwald, O. D. Gurcan, T. S. Hahm, A. E. Hubbard, E. S. Marmar, C. J. McDevitt, and D. G. Whyte, Phys. Rev. Lett. **106**, 215001 (2011).

[33] S. M. Kaye, W. M. Solomon, , R. E. Bell, B. P. LeBlanc, F. M. Levinton, J. E. Menard, G. Rewoldt, S. A. Sabbagh, W. Wang, and H. Yuh, Nucl. Fusion **49**, 045010 (2009).

[34] Y. Kosuga, P. H. Diamond, and O. D. Gurcan, Phys. Plasmas **17**, 102313 (2010).

[35] J.-K. Park, A. H. Boozer, and A. H. Glasser, Phys. Plasmas **14**, 052110 (2007).

[36] J. E. Menard, R. E. Bell, D. A. Gates, S. P. Gerhardt, J.-K. Park, S. A. Sabbagh, J. W. Berkery, A. Egan, J. Kallman, S. M. Kaye, B. LeBlanc, Y. Q. Liu, A. Sontag, D. Swanson, H. Yuh, W. Zhu, and the NSTX Research Team, Nucl. Fusion **50**, 045008 (2010).

[37] S. P. Gerhardt, J. E. Menard, J.-K. Park, R. Bell, D. A. Gates, B. P. LeBlanc, S. A. Sabbagh, and H. Yuh, Plasma Phys. Control. Fusion **52**, 104003 (2010).

[38] J.-K. Park, A. H. Boozer, J. E. Menard, A. M. Garofalo, M. J. Schaffer, R. J. Hawryluk, S. M. Kaye, S. P. Gerhardt, S. A. Sabbagh, and the NSTX team, Phys. Plasmas **16**, 056115 (2009).

[39] A. M. Garofalo, W. M. Solomon, J.-K. Park, K. H. Burrell, J. C. DeBoo, M. J. Lanctot, G. R. McKee, H. Reimerdes, L. Schmitz, M. J. Schaffer, and P. B. Snyder, Nucl. Fusion **51**, 083018 (2011).

[40] K. H. Burrell, A. M. Garofalo, W. M. Solomon, M. E. Fenstermacher, T. H. Osborne, J.-K. Park, M. J. Schaffer, and P. B. Snyder, Phys. Plasmas **19**, 056117 (2012).

The Princeton Plasma Physics Laboratory is operated
by Princeton University under contract
with the U.S. Department of Energy.

Information Services
Princeton Plasma Physics Laboratory
P.O. Box 451
Princeton, NJ 08543

Phone: 609-243-2245
Fax: 609-243-2751
e-mail: pppl_info@pppl.gov
Internet Address: http://www.pppl.gov